IJESRT

INTERNATIONAL JOURNAL OF ENGINEERING SCIENCES & RESEARCH TECHNOLOGY

DEVELOPMENT OF AN ELECTROLYTIC CATION EXCHANGE MODULE (E-CEM) FOR THE SIMULTANEOUS EXTRACTION OF CARBON DIOXIDE FROM SEAWATER AND HYDROGEN GAS GENERATION: EFFECTS OF STRONG CATION EXCHANGE RESIN CAPACITY ON CARBON DIOXIDE PRODUCTION EFFICIENCY

Heather D. Willauer*, Felice DiMascio, Dennis R. Hardy, Frederick W. Williams
* Materials Science & Technology Division, Naval Research Laboratory, 4555 Overlook Avenue SW,Washington, DC 20375.
Office of Naval Research, Arlington, VA 22203.
NOVA Research Inc., 1900 Elkin Street, Alexandria, VA 22308.
Chemistry Division, Naval Research Laboratory, 4555 Overlook Avenue SW, Washington, DC 20375.

ABSTRACT

A novel and innovative electrolytic cation exchange process has been developed to extract large quantities of CO_2 in the form of bicarbonate and carbonate from natural seawater, and to simultaneously produce H_2 gas in quantities and ratios intended for possible future production of hydrocarbons. However this process has been limited by its energy efficiency and carbon dioxide production efficiency caused by the amount of time needed to re-establish equilibrium conditions in the module after a polarity reversal cycle. To shorten the re-equilibrium times and improve carbon dioxide recovery, the strong cation exchange resin capacity in the electrode compartments was reduced from 2.1 eq/L to 1 eq/L. This 50% reduction in capacity resulted in 33% improvement in production time of CO_2. In addition, quantitative gas sampling analyses of CO_2 confirmed the relationship between seawater salinity, seawater carbonate concentration, and seawater temperature on ease of CO_2 degassing from seawater.

KEYWORDS: electrolytic cation exchange module (E-CEM), carbon dioxide, bicarbonate, ion exchange, membrane, seawater.

INTRODUCTION

Solutions to solving global increases in anthropogenic levels of carbon dioxide (CO_2) in the earth's atmosphere have led to extensive research in the development of carbon capture and storage (CCS) technologies.[1-4] The long term effects of storage in geological formations and in the ocean remain unknown and as a result there is increasing emphasis on utilizing the CO_2 in industrial processes.[2,3] Currently CO_2 is commercially used by the petroleum and gas industry for the enhanced recovery of oil, gas and methane.[2] CO_2 is used in the food industry to carbonate beverages and as a protective atmosphere for food. It is also used in fire-extinguishers, as an inerting atmosphere for welding, in the handling of flammable materials, and as a solvent for dry cleaning and separations.[3] While such commercial CO_2 applications are in demand, they simply do not utilize enough CO_2 to have a significant impact on reducing CO_2 emissions.[3]

CO_2 fixation in microalgae and its conversion to chemicals and polymers, offers yet more commercial applications that will help to reduce CO_2 emissions and generate revenue to offset the cost of capture and separation technologies.[2,3] However these processes require the CO_2 to be extremely pure.[2,3] The CO_2 from flue and stack gases contains SO_x that greatly restricts microalgae growth and stops it all together at 50 ppm.[3] Catalysts used in chemical conversion and reduction of CO_2 will be poisoned rapidly by these impurities.[1,2] In addition, proven scalable approaches to produce usable chemical fuels from CO_2 (methanol and olefins) require a source of hydrogen.[2,3,5] Since CO_2 purity and the need for hydrogen are issues in chemical conversion of CO_2 to useable chemicals and fuels, perhaps a cleaner more general approach to the removal of anthropogenic CO_2 from the environment could be useful.

The world's oceans contain approximately 100 mg/L of total carbon dioxide $[CO_2]_T$ of which 2 to 3 percent is dissolved CO_2 gas in the form of carbonic acid, 1% is carbonate and the remaining 96 to 97% is bound as bicarbonate.[6,7] Comparing the seawater concentration on a weight per volume basis (w/v) to that of a stack gas (about 300 mg/L) and air (about 0.77 mg/L)[1] strongly suggests the world's oceans could be the key to a more general, practical, and cleaner approach to removing the anthropogenic gas from the environment.

Willauer et al. have modified and scaled-up continuous electrodionization (CEDI) technology to function as a novel electrolytic cation exchange module (E-CEM) for the simultaneous extraction of carbon dioxide from seawater and the production of hydrogen.[8] This electrochemical approach is different from bipolar membrane electrodialysis (BPMED) used by Eisaman and coworkers to extract only CO_2 from instant ocean.[9] The BPMED module was configured to use low current, strong acid electrode solutions, and a combination of bipolar membranes, and individual cation ion and anion exchange membranes. The process described within is different from Yamasaki's process that extracts only CO_2 from carbonate solutions created from absorption of CO_2 from a flue gas stream that is passed through a sodium hydroxide solution. The electrodialysis module used low current, strong acid electrode solutions, and a combination bipolar membranes and cation exchange membranes.[10] The process is also different from the one previously reported by our group that used strong cation exchange resin with a capacity of 2.1 eq/L.[8]

This latest modification has been named the electrolytic cation exchange module (E-CEM) and it indirectly separates and purifies CO_2 from seawater as illustrated in eq 1.

$$HCO_3^- + CO_3^{-2} + H^+ \rightleftarrows H_2CO_3 \rightleftarrows H_2O + CO_2\,(g)\uparrow \qquad\qquad (1)$$
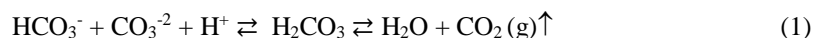
The addition of protons to seawater, produced in the E-CEM, causes the bicarbonate and carbonate to re-equilibrate to carbonic acid at seawater pH less than or equal to 6. The CO_2 gas is vacuum stripped via a gas membrane, producing a stream of essentially pure CO_2 gas with traces of water vapor, nitrogen, and oxygen. The acidification of seawater below pH 6 has been the basis for standard ocean $[CO_2]_T$ measurements for over 25 years.[11]

In our previous work, the initial scale-up and integration of the E-CEM into a skid platform demonstrated the feasibility of the electrochemical concept for the simultaneous extraction of CO_2 from seawater and production of H_2.[8] At seawater flowrates of 1900 mL/min, 92% of $[CO_2]_T$ was extracted from the natural seawater at a pH $\leq$ 4. In addition, a set of times were ascertained to provide operational parameters for the process. These studies provided data needed to purse different E-CEM designs aimed at establishing faster equilibrium conditions for future modules during polarity reversal and to improve energy efficiencies.

Polarity reversal was designed into the E-CEM process at regular intervals, called polarity cycles, to overcomer major challenges associated with mineral deposition on the electrode surface that occurs in the high pH environment of the cathode compartment. Mineral deposition leads to higher electrical resistance in the module, a loss in electrical efficiencies, and the potential for damaging the module from restricting flow in the cathode compartment. Polarity reversal is a common practice in the Electrodialysis Reversal (EDR) process to desalinate brackish ground and surface waters.[12] The objective of this study is to increase the CO_2 production efficiency of the E-CEM by reducing the amount of time needed after polarity reversal for the ion exchange resin in the electrode compartments to re-establish equilibrium conditions and the effluent seawater to drop below pH 6 to change the ionically bound carbonate and bicarbonate to CO_2 gas. For a defined current and set of operating conditions, the original scaled-up E-CEM took approximately 30 minutes to reach equilibrium after a polarity cycle. A reduction in this equilibration time will increase the total amount of CO_2 extracted per process unit time, and reduce the energy demands associated with re-equilibrating the module. This is essential to the overall long term economic feasibility of utilizing the process for carbon capture from seawater.

The first approach to increasing CO_2 production efficiency of the module was to reduce the strong cation exchange resin capacity in the electrode compartments from 2.1 eq/L to 1 eq/L. The E-CEM's performance was evaluated by measuring the effluent seawater pH, current, voltage, and electrical resistance profiles as a function of polarity cycle

and comparing them to those of the original scaled-up E-CEM. In addition, relationships were established between natural seawater salinity, seawater carbonate concentration, and seawater temperature on the ease of CO_2 degassing from seawater.

EXPERIMENTAL METHODOLOGY

Electrolytic Cation Exchange Module (E-CEM). Figure 1 shows two schematics (a and b) that describe the differences between the original E-CEM configuration (a) and the E-CEM configuration (b) evaluated in this study. The E-CEMs are standard commercially available electrodeionization cells (Ionpure LX-X Module) modified to function as an electrolytic cation exchange module for the simultaneous extraction of H_2 and CO_2 from seawater. The major components of the E-CEMs include a center compartment, electrode compartments (cathode and anode capable of reversing polarities), and two cation-permeable membranes which separate the three compartments. Polyethylene extruded cation-permeable heterogeneous monolithic membranes incorporate cross-linked polymer with sulfonic acid groups attached. The acid functionality provides discrete channels for cations to migrate through the polymer matrix while blocking the passage of anions. Inert plastic particles were used in the center compartment to serve as a support structure for the membranes. In this central compartment, the ions (Na^+/H^+) exchange in the liquid phase. In addition, Figure 1 shows that the electrode compartments contain cation exchange resin. The cation exchange resin, its amount, and capacity differ between original E-CEM (a) and the E-CEM (b) used in this evaluation. The original E-CEM (a) contained 100% strong cation exchange resin from Rohm & Haas (IR-120) in both electrode compartments and its capacity is 2.1 eq/L. In the modified module (Figure 1b.) each electrode compartment is configured to contain 50% less ion exchange capacity. However, each electrode compartments is configured differently to achieve this objective. In Figure 1, the electrode compartments of the module are defined as side B and side A for each module. In the module used in this evaluation Figure 1b, side B contains 100% strong acid ion exchange resin with a capacity of 1 eq/L. Side A contains 50% less of the strong acid cation exchange resin that was used in the original module (2.1 eq/L). This resin is mixed with 50% inert material to fill the compartment. Polarity A and B define the electrode compartment side of the module (side A or B) from Figure 1. Polarity A and polarity B designate the electrode compartment (side A or side B) that is functioning as the anode during the polarity cycle (modules pictured operating as polarity B).

The resins and membranes used in the modules are typically used for years in commercial water treatment electrolysis processes. Our water filtration and current densities are well within the specifications of all products used to construct the module. After 4 years of intermittent use, we have not seen any degradation or deterioration of the resin or membranes used to construct the modules. The anode and cathode titanium electrodes were coated with platinum and had an electrode active area of 497 cm^2.

Feed Through the Electrolytic Cation Exchange Module (E-CEM). In this continuous flow process, seawater is passed through the center compartment of the E-CEM (Figure 1) at a flow rate of 0.5 gal/min (1900 mL/min), while fresh water is passed through the anode and cathode compartments each at 0.06 gal/min (230 mL/min). Direct current (DC) is used to produce H^+ ions, O_2, and electrons at the anode. These H^+ ions migrated from the surface of the anode, through the cation-permeable membrane, and into the center compartment where they replace the Na^+ ions in the seawater to acidify the seawater. The Na^+ ions are transferred through the membrane closest to the cathode and removed from the seawater. Simultaneously at the cathode OH^- ions and H_2 are produced and electrons are consumed. The positive ions removed from the seawater (sodium being at the highest concentration) provide electrical neutrality in the cathode compartment to form a basic aqueous solution composed primarily of sodium hydroxide. The fresh water used in the module is produced from the natural Key West (KW) seawater by a reverse osmosis system (RO). The fresh water had a conductivity of less than 200 μS/cm and measured approximately pH 7. Magnesium and calcium ions from the seawater also migrate to the cathode compartment and produce scale on the cathode over time. The effects of this scale are mitigated by cyclically reversing the module's polarity.[12]

Carbon Capture Skid and Procedure. Since natural Key West seawater was used, the work was performed at the Naval Research Laboratory's Corrosion Laboratory at Key West, FL to evaluate the E-CEM's performance. The module was incorporated into a portable skid along with an RO unit, power supply, pumps, a membrane contactor

carbon dioxide gas recovery system, hydrogen gas vacuum tower, and gas analyzer to form a carbon and hydrogen capture system, all operated by a control logic capable of maintaining automatic operation safely on a continual basis. A process flow diagram and labeled photograph of the carbon capture skid have previously been reported.[8] Seawater was supplied to the skid by an in-house 40 psi supply line. The water was filtered by two spin-down filters in series (100 μm and 30 μm). After filtration, a portion of the seawater was sent to an 11 gallon high density polyethylene container that functions as the seawater feed container. Before the seawater in the seawater feed tank was fed to the center compartment of the E-CEM at 0.5 gallon/minute (1900 mL/min), it was pumped through a 5 μm filter cartridge. The other portion of the seawater supply was fed through a 5 μm filter cartridge to the RO system for processing. The RO system was an EPRO-1000SW from Crane Environmental, Inc. (Venice, FL) that is capable of producing 0.7 gallons per minute (1000 gallons per day) of permeate (fresh water quality from seawater at a conductivity of approximately 200 μS/cm). This water was stored in an 11 gallon polyethylene container that is specified as the RO feed container. This water was the feed water to the electrode compartments of the E-CEM at a total flow rate of 0.12 gallon/minute (460 mL/min). The flow was split within the E-CEM resulting in electrode compartment flow rates of 0.06 gallon/minute (230 mL/min) to each electrode compartment.

A Mastech HY3030EX 0-30 amp, 0-30 volt high-current, regulated DC power supply was used to supply the current to the E-CEM electrodes. The seawater pH changed as a function of applied current to the E-CEM. Effluent seawater pH was monitored continuously using a standard combination electrode as it exited the center compartment of the module. Vision 290 Unitronics hardware and software were used to control the system components (RO, E-CEM, well pump, vacuum towers, vacuum pumps, solenoid valves, and power supply) so they operated and functioned together as an integrated unit on a continual automated basis, with limited operator control required. The CO_2 gas from the effluent acidified seawater flowing at 0.5 gallons/minute was vacuum stripped using a commercial membrane contactor (Liqui-Cel® 2.5 x 8 polyethylene hollow fiber membrane contactor (Membrana-Charlotte). The $[CO_2]_T$ content of the acidified effluent seawater was measured by coulometry (UIC Inc, Joliet, IL 60436) after contact with the membrane contactor to determine the efficiency of the extraction method.[11] The $[CO_2]_T$ content of the natural Key West seawater before acidification was measured to be approximately 100 mg/L. Simultaneously, a standard purpose-built hydrogen gas vacuum tower processed the water from the acting cathode compartment of the module as it liberated H_2 gas. The H_2 gas was measured qualitatively throughout the operation by a standard Honeywell gas analyzer (7866 digital gas analyzer), as was the CO_2.

TRI Air Testing Inc performed separate evaluations of gas samples of CO_2 and H_2 collected during the test evaluation.

RESULTS AND DISCUSSION
The E-CEM takes advantage of continuous electrodeionization (CEDI) principles of removing ionizable species from liquids by manipulating their ionic transport properties using an applied electrical potential, ion exchange resins, and semipermeable ion exchange membranes as electrically active media.[12-17] In the E-CEM process depicted in Figure 1 (modules pictured operating as polarity B), sodium chloride (NaCl) is used to represent seawater and HCl is used to represent the acidified effluent seawater. When direct current is applied to the module, H^+ ions and O_2 gas are generated at the anode by the oxidation of the anolyte RO water. The amount of H^+ generated by the anode is proportional to the applied electrical current, which follows Faraday's law. The anode and cathode reactions to theoretically determine the amount of H^+, OH^-, H_2, and O_2 produced per amp-second of current passed through the electrodes has been previously detailed by Willauer et al.[18,19] The O_2 gas is flushed from the anode compartment with the flow of the anolyte (deionized water). The H^+ ions are driven from the surface of the anode, through the cation-permeable membrane, and into the center compartment where they replaced the Na^+ in the flowing seawater. This causes the effluent seawater to be acidified without the need for any additional chemicals. At a seawater pH less than or equal to 6, the bicarbonate and carbonate in the seawater are re-equilibrated to carbonic acid (eq 1). The Na^+ ions in the center compartment are passed through the membrane closest to the cathode to produce primarily sodium hydroxide and H_2 gas in the cathode compartment. The NaOH and H_2 gas are continuously flushed from the cathode compartment with the flow of the catholyte (RO water). The CO_2 from the carbonic acid in the acidified seawater is vacuum stripped by a gas permeable membrane contactor. The acidified seawater is recombined with the solutions from the cathode and anode compartment.

When the polarity is reversed, the ion exchange resin in the electrode compartment functioning as the anode is in the sodium Na^+ form, the H^+ ions generated at the anode exchange on the resin and releases the Na^+ ions. The Na^+ ions then migrate through the cation exchange membrane and into the center compartment. The migrating Na^+ ions pass through the cation exchange membrane at the electrode now acting as the cathode and exchange on the resin to convert all the resin in that compartment to the sodium form. Equilibrium conditions are re-established during the polarity cycle when all the resin in the compartment now acting as the anode is regenerated back into the hydrogen form and all the resin in the cathode is regenerated back into the sodium form. This allows more H^+ ions to pass through the membrane closest to the anode to reduce the seawater pH below 6.

Figure 1a shows the original scaled-up E-CEM contained 100% strong cation exchange resin at a capacity of 2.1 eq/L in both electrode compartments. This module took approximately 30 minutes to reach equilibrium after the module's polarity was reversed. To reduce the time needed after polarity reversal for the ion exchange resin in the electrode compartments to re-establish equilibrium conditions, the capacity of the ion exchange resin in the compartments was reduced from 2.1 eq/L to 1.0 eq/L.

Figures 2a and 2b compare the pH profiles measured as a function of time for a defined electrode compartment side (side A or B) at an applied module current of 20 Amps. Figure 2a shows 7 polarity cycles for Polarity A. The electrode compartment acting as the anode during these 7 cycles was filled with a mixture containing 50% cation exchange resin with a capacity of 2.1 eq/L and 50% inert material. The cathode compartment was filled with cation exchange resin with a capacity of 1.0 eq/L. The initial pH of the influent Key West seawater during this evaluation was 8.18 ± 0.02. The Figure shows that after approximately 20 minutes have passed the pH of the effluent seawater dropped below 6. This is a function of the cation exchange resin capacity, volume ($215 \ cm^3$), and applied current. After 26 minutes the pH of the effluent seawater measured below 4. Previous results have indicated that 92% of the CO_2 is recoverable at a seawater pH below 4.5.[8,18,19]

Figure 2b indicates that similar pH profiles are measured as a function of time for Polarity B at an applied module current of 20 Amps. During these cycles the compartment acting as the anode contained 100% cation exchange resin with the capacity of 1 eq/L. These results verify that two completely different approaches of reducing the ion exchange capacities in the electrode compartments reduced the seawater pH below 6.

The pH profiles in Figures 2a and 2b are averaged for a given polarity and compared to the average profiles obtained for the original E-CEM. Figure 3 shows that for a defined current, the modified E-CEM reduces the effluent seawater equilibrium pH to 6 in approximately 20 minutes compared to the original E-CEM that takes 30 minutes. This improves the production time of CO_2 by 33% over the original module. Therefore a reduction in ion exchange capacity allows the equilibrium conditions to be re-established faster in the module. This increase in production is crucial to the overall process feasibility of scaling and utilizing the process for carbon capture from seawater.

Figure 4 compares the average of 7 electrical resistances (voltage divided by amperage) profiles as a function of time for Polarity A and B of the modified module. Comparing the averages of both cycles shows that the measured resistance decreases by approximately 31% for Polarity A and only 20% for Polarity B over the first 45 minutes of the cycle. Both cycles also indicate an increase in resistance 45 minutes into the cycle. This is consistent with operational parameters ascertained for the original module. The greater decrease in electrical resistance during Polarity A may be explained by the conductivity of the ion exchange resin in the electrode compartment acting as the anode.

The conductivity (κ) in the module is the sum of all the individual components involved in ion transport. Figure 5 shows a total of 5 components responsible for the conductivity of both the original module and the modified module. The sum of these components is given in equation 2

$$\kappa = \kappa_1 + \kappa_2 + \kappa_3 + \kappa_4 + \kappa_5 \qquad (2)$$

where κ_1 and κ_5 are the conductivities of the cation exchange resin and reverse osmosis permeate mixture in the electrode compartments, κ_2 and κ_4 are the conductivity of the cation exchange membranes, and κ_3 is the conductivity of the seawater and inert pellet mixture in the center compartment.

κ_1 and κ_5 are dependent on the characteristics of the cation exchange resin, particularly ion exchange capacity and DVB (divinyl-benzene) crosslinkage percentage. This will vary from one ionic form to another. κ_2 and κ_4 are fairly constant, while κ_3 is dependent on the ratio and particle size of the inert pellets. The electrical resistance 'R' (Ω) is related to the conductivity of the module by equation 3

$$R = x/A\kappa \qquad\qquad (3)$$

where x is the distance between the electrodes in cm and A is the electrode effective area in cm^2. The area A may be expressed as a function of the electrode length (y) and width (z) as given in equation 4 and provided as the effective electrode active area, 497 cm^2 (each).

$$A = (y)(z) \qquad\qquad (4)$$

The electrical resistance of the module is monitored as a function of the current and voltage supplied to the module during a defined polarity cycle. Table 1 is the calculated average conductivity values for Polarity A and B over 7 cycles. The Table indicates that during polarity A the ion exchange material in the anode becomes more conductive at an average of 15 minutes into the cycle. At this point the pH begins to fall below 6 and all the ion exchange material is regenerated back into the hydrogen form and all the resin in the cathode compartment is regenerated back into the sodium form. The conductivity reaches a maximum of 0.0028 at an average of 30 minutes into the cycle.

Similarly during polarity B the ion exchange material in the anode becomes more conductive at an average of 15 minutes into the cycle. The conductivity is initially higher in this compartment upon polarity reversal, but only reaches a maximum of 0.0025 at 25 minutes. The difference in conductivity found between each polarity cycle indicates that the 50/50 mixture of cation ion exchange resin (2.1 eq) and inert material has the most conductivity and produces the least amount of resistance in the module over an average 45 minute cycle. This decrease in resistance results in a 7% increase in power efficiency over the average 45 minute cycle. Thus the average power during polarity A is 540 watts compared to 581 watts during polarity B.

Figure 6 compares the average resistance as a function of time of the original E-CEM and the modified E-CEM. For the purposes of this comparison, the original E-CEM was tested during this study to establish a set of baseline conditions for E-CEM comparison. Figure 6 shows the average resistance for both polarity cycles of the original E-CEM is approximately 0.96. This value is 35% less than the average resistance of the modified E-CEM during polarity A (50/50 ion exchange and inert material) and 37% less than the average resistance of polarity B (50% less ion exchange capacity 1.0 eq/L). The greater resistance in the modified E-CEM is a result of the conductivity of the ion exchange material in the electrode compartments. The average conductivity of the original module was measured to be 0.0038 compared to 0.0024 of the modified module. This 37% reduction in conductivity results in a 37% increase in module resistance. This increase in module resistance results in an increase in the average power requirements from 387 watts needed for the original module to 540 watts (polarity A) and 581 watts (polarity B) needed for the modified module.

Willauer et al. have previously detailed how Faraday's constant 96,487 A-second and the anode and cathode reactions within the E-CEM (Figure 1) are used to theoretically determine the amount of H^+, OH^-, H_2, and O_2 produced per amp-second of current passed through the electrodes in the process.[18,19] Equation 5 shows the theoretical maximum molar amount of H_2 gas derived at a current of 20 A within the E-CEM

$$\left(\frac{1/2 \text{ mole } H_2}{96{,}487 \text{ A-sec}}\right)\left(\frac{60 \text{ sec}}{\text{min}}\right)(20 \text{ A}) = 0.0062 \frac{\text{mole } H_2}{\text{min}} \qquad (5)$$

The 0.0062 moles H_2/min theoretically possible is equivalent to 0.0083 m^3/hour H_2. The average power requirements for the original E-CEM was 0.387 kWh/h compared to the 0.540 kWh/h and 0.581 kWh/h values found for the modified module. The hydrogen power consumption values at 100% efficiency are estimated to range from 46.6 kWh/m^3 (518 kWh/kg) for the original E-CEM to 65.1 kWh/m^3 (724 kWh/kg) (polarity A) to 70 kWh/m^3 H_2 (778 kWh/kg) (polarity B) for the modified E-CEM.

The estimated H_2 power consumption values for the E-CEM process are compared to the NEL commercial electrolysis processes. NEL reports power consumption values ranging from 3.8 to 4.4 kWh/$m^3 H_2$ (42.3 kWh/kg H_2 to 48.9 kWh/kg H_2) for their water electrolyzer cell stacks.[20] To produce 0.0083 m^3/H_2 at 100% efficiency by the NEL process it would take approximately 0.031 kWh/h to 0.036 kWh/h of power. The E-CEM process needs 12 to 17 times more power to produce H_2 gas than the traditional commercial water electrolysis process.

Though modifying the E-CEM by reducing the conductivity of the ion exchange material in the electrode compartments improved the production time of CO_2 by 33% over the original module, further modifications to the E-CEM must be made so the process can compete with commercial electrolysis. Since commercial off the shelf CEDI endblocks were used in these evaluations, key parameters discussed in equations 2, 3, and 4 cannot be fully adjusted to measure and determine their impact on increasing CO_2 production time and reducing power consumption for H_2 production. The results of this study will be used to purse custom design modifications to further improve CO_2 production time and reduce overall power consumption.

Willauer, et al have recently ascertained from both the laboratory feasibility tests and scaled-up evaluations that CO_2 more readily degasses from seawater solutions higher in salt concentration and carbonate concentration at pH below 6.[8,19] In Table 2 the results are given for three separate evaluations of the original E-CEM process at NRL Key West during January 2011, April 2011, and January 2012. The first evaluation in January 2011 of the scaled-up carbon capture system found that approximately 48% of the $[CO_2]_T$ spontaneously degassed from the effluent seawater at pH 3.63. Further improvements in degassing the seawater were not achieved using different stripper columns to produce larger surface area for seawater degassing by a 600 mL/min vacuum pump operating at a vacuum of 12 inches of Hg.

During the April 2011 evaluation a Liqui-Cel polyethylene hollow fiber membrane contactor was tested as a method to increase seawater surface area and thus improve in CO_2 degassing efficiency from the seawater at pH below 6.[21] Gas permeable membranes work on the principle of dissolved gases (in this case carbon dioxide) diffusing across the membrane through the pores as a function of differential partial gas pressures. As a result, these membranes are used in a variety of near atmospheric pressure applications such water purification, blood oxygenation, and artificial lung devices.[22-25] They have also found utility in high pressure applications involving beverage carbonation.[26,27] Table 2 shows $[CO_2]_T$ degassing between pH 3 and 4 increased from 48% to 92%. Since the CO_2 gas recovered is contaminated by the oil in the rotary vane pump, a diaphragm pump capable of 25 to 30 inches of Hg was purchased and used in the January 2012 evaluations of $[CO_2]_T$ recovery. During the evaluation it was found that only 63 to 66% of $[CO_2]_T$ below pH of 4 could be recovered using a vacuum of approximately 29.1 inches of Hg. This percentage was improved to 85% when the vacuum was increased to 30.5 inches of Hg using a rotary vane pump with a cold trap.

The different $[CO_2]_T$ recovery between the months of January and April may be explained by the decrease in bulk temperature of the influent seawater and its decrease in salinity as a function of decrease in seawater temperature. It is well known that CO_2 gas solubility is reduced in aqueous salt solutions compared to deionized water solutions.[28-30] In addition, CO_2 gas solubility decreases with increasing liquid temperatures.[31] Figure 7 illustrates the difference in resistance between the different tests series conducted in January, April, and August. The average seawater temperature in January, April, and August was 22 °C, 25 °C, and 31 °C. The greatest difference in resistance profiles

is shown for the data measured in the month of January 2011 and January 2012. At lower seawater temperatures the electrical conductivity of the seawater decreases as the salinity decreases due to the lack of evaporation of the surface waters at colder temperatures. This leads to an increase in the electrical resistance within the module. In addition, under these conditions greater seawater surface area and greater vacuum requirements are needed for better CO_2 degassing efficiencies via vacuum membrane contactors.

In addition to measuring $[CO_2]_T$ content of seawater by coulometery during this evaluation, a Honeywell 7866 digital gas analyzer with a thermal conductivity detector was used to measure the amount of $[CO_2]_T$ gas evolved from the membrane contactor at 29.1 inches of Hg. From the Table 2, the $[CO_2]_T$ content measured in the gas samples for a given pH of 3.67 and 3.46 was 66% and 63% respectively. Similarly the seawater samples collected at those pH measured a loss of $[CO_2]_T$ of 63% and 66% by coulometery. These results indicate an excellent correlation between two different measuring techniques of $[CO_2]_T$ content. To further substantiate these results, gas samples were collected at 3.44 and 3.66 and sent to TRI Air Testing Inc. Table 2 shows their analysis strongly supports results found by real time gas analysis and coulometery at seawater pH less than 4.

CONCLUSIONS

Based on the evaluation of the original E-CEM performance, a second module was modified to contain less ion exchange capacity in the electrode compartments. The evaluation of this new design found CO_2 production improved 33% by reducing the amount of time it takes for the effluent seawater equilibrium pH to reach 6 after a change in polarity. Evaluation of the resistance profiles and conductivity of the materials used in the electrode compartments found that the 50/50 mixture of cation ion exchange resin (2.1 eq) and inert material had the most conductivity and produced the least amount of resistance in the modified E-CEM. This decrease in resistance resulted in a 7% increase in power efficiency over a cycle. Comparing the resistance profiles and conductivity of both the original E-CEM and the modified E-CEM shows that the original module requires less average power to operate over a polarity cycle.

Quantitative measurements of $[CO_2]_T$ degassed from seawater correlated well with the quantitative difference in $[CO_2]_T$ measured in the seawater by coulometry. These quantitative measurements along with resistance profiles confirm that CO_2 degassing at seawater pH below 6 is dependent on seawater temperature, salinity, and carbonate concentration.

Finally, the E-CEM design evaluated in these studies proved to be even less efficient in energy consumption than the original E-CEM, and the overall E-CEM was 12 to 17 times less efficient in H_2 gas production from the traditional commercial water electrolysis process. However these studies have laid the groundwork needed to pursue future E-CEM design modifications. These modifications will be based on manipulating key parameters associated with the overall conductivity of the E-CEM. These parameters along with an understanding of CO_2 degassing dependence on seawater composition and temperature will lead to future E-CEM designs tailored towards maximizing both CO_2 extraction and H_2 production at energy efficiencies closer to the 3.8 to 4.4 kWh/m^{3}H$_2$ (42.3 kWh/kg H_2 to 48.9 kWh/kg H_2) currently reported for commercial water electrolysis units.

REFERENCES

[1] Goeppert, A.; Czaun, M.; Surya Prakash, G. K.; Olah, G. A. Air as the renewable carbon source of the future: an overview of CO_2 capture from the atmosphere. *Energy Environ. Sci.*, **2012,** *5,* 7346-7352.
[2] Markewitz, P.; Kuchshinrichs, W.; Leitner, W.; Linssen, J.; Zapp, P.; Bongartz, R.; Schreiber, A.; Müller T. E. Worldwide innovations in the development of carbon capture technologies and the utilization of CO_2. *Energy Environ. Sci.*, **2012,** *5,* 7281-7305.
[3] Huang, C-H.; Tan, C-S.; A review CO_2 utilization. *Aerosol and Air Quality Research*, **2014,** *14*, 480-499.

[4] MacDowell, N.; Florin, N.; Buchard, A.; Hallett, J.; Galindo, A.; Jackson, G.; Adjiman, C. S.; Williams, C. K.; Shah, N.; Fennell, P. An overview of CO_2 capture technologies. *Energy Environ. Sci.* **2010,** *3,* 1645-1669.

[5] Peng, Y. P.; Yeh, Y. T.; Wang, P. Y.; Huang, C. P. A solar cell driven electrochemical process for the concurrent reduction of carbon dioxide and degradation of azo dye in dilute $KHCO_3$ electrolyte, *Separation and Purification Technology* **2013,** *117,* 3-11.

[6] Takahashi, T.; Broecker, W. S.; Bainbridge, A. E. The Alkalinity and Total Carbon Dioxide Concentration in the World Oceans. In *Carbon Cycle Modelling*; SCOPE: New York, 1981; Vol. *16*, pp 271-286.

[7] Takahashi, T.; Broecker, W. S.; Werner, S. R.; Bainbridge, A. E. Carbonate Chemistry of the Surface of the Waters of the World Oceans. In *Isotope Marine Chemistry*; Goldberg, E. D., Horibe, Y., Katsuko, S., Eds.; Uchida Rokakuho: Tokyo, Japan, 1980; pp 291-326.

[8] Willauer, H. D.; DiMascio, F.; Williams, F. W. Feasibility of CO_2 extraction from seawater and simultaneous hydrogen gas generation using a novel and robust electrolytic cation exchange module based on continuous electrodeionization technology, *I&EC* **2014,** *53*, 12192-12200.

[9] Eisaman, M. D.; Parajuly, K.; Tuganov, A.; Eldershaw, C.; Chang, N.; Littau, K. A. CO2 Extraction from seawater using bipolar membrane electrodialysis. *Energy Environ. Sci.* **2012,** *5,* 7346-7352.

[10] Lizuka,, A.; Hashimoto, K.; Nagasawa, H.; Kumagai K.; Yanagisawa, Y.; Yamasaki, A. Carbon dioxide recovery from carbonate solutions using bipolar membrane electrodialysis. *Separation and Purification Technology* **2012,** *101*, 49-59.

[11] Johnson, K. M., King, A. E., Sieburth, J. Coulometric TCO2 Analyses for Marine Studies: An Introduction. Mar. Chem. 1985, 16, 61.

[12] Dermentzis, K. Continuous electrodeionization through electrostatic shielding. *Electrochim. Acta* **2008,** *53*, 2953-2962.

[13] Fedorenko, V. I. Ultrapure water production using continuous electrodeionization. *Pharm. Chem. J.* **2003,** *37*, 157-160.

[14] Lounis, A.; Setti, L.; Djennane, A.; Melikchi, R. Separation of Molybdenum-Uranium by a process combining ion exchange resin and membranes. *J. Appl. Sci.* **2007,** *4*, 1963-1967.

[15] Wood, J.; Gifford, J.; Arba, J.; Shaw, M. Production of ultrapure water by continuous electrodeionization. *Desalination* **2010,** *250*, 973-976.

[16] Keramati, N.; Moheb, A.; Ehsani, M. R. Effects of operating parameters on NaOH recovery from waste stream of Merox tower using membrane systems: Electrodialysis and electrodeionization processes. *Desalination* **2010,** *259*, 97-102.

[17] Kurup, A. S.; Ho, T.; Hestekin J. A. Simulation and optimal design of electrodeionization process: Separation of multicomponent electrolyte solution. *Ind. Eng. Res.* **2009,** *48*, 9268-9277.

[18] Willauer, H. D.; DiMascio, F.; Hardy, D. R.; Lewis, M. K.; Williams, F. W. Development of an Electrochemical Acidification Cell for the Recovery of CO_2 and H_2 from Seawater. *Ind. Eng. Chem. Res.* **2011,** *50,* 9876-9882.

[19] Willauer, H. D.; DiMascio, F.; Hardy, D. R.; Lewis, M. K.; Williams, F. W. Development of an Electrochemical Acidification Cell for the Recovery of CO2 and H2 from Seawater II. Evaluation of the cell by Natural Seawater. *Ind. Eng. Chem. Res.* **2012,** *51,* 11254-11260.

[20] NEL Hydrogen http://www.nel-hydrogen.com/Accessed June 18, 2015.

[21] Willauer, H. Dl; DiMascio, F.; Hardy, H. D.; Lewis, M. K.; Williams, F. W. Method for the continuous of carbon dioxide from acidified seawater," PN US 8,663,365 March 4, 2014.

[22] Bhaumik, D.; Majumdar, S.; Fan, Q.; Sirkar, K. K. Hollow Fiber Membrane Degassing in Ultrapure Water and Microbiocontamination. *J. Membr. Sci.* **2004,** *235,* 31.

[23] Lund, L. W.; Hattler, B. G.; Federspiel, W. J. Gas Permeance Measurement of Hollow Fiber Membranes in Gas-Liquid Environment. *AIChE J.* **2002,** *48,* 635.

[24] Lund L. W.; Federspiel, W. J.; Hattler, B. G. Gas Permeability of Hollow Fiber Membranes in a Gas-Liquid System. *J. Membr. Sci.* **1996,** *117,* 207.

[25] Eash, H. J.; Jones, H. M.; Hattler, B. G.; Federspiel, W. J. Evaluation of Plasma Resistant Hollow Fiber Membranes for Artificial Lungs. *ASAIO J.* **2004,** *50,* 491.

[26] Bosko, R. S. Hollow Fiber Carbonation. US Patent 6,712,342, March 20, 2004.

[27] Gabelman, A.; Hwang, S-T. Hollow Fiber Membrane Contactors. *J. Membr. Sci.* **1999,** *159,* 61.

[28] Follows, M. J.; Ito, T.; Dutkiewics, S. On the solution of the carbonate chemistry system in ocean biogeochemistry models. *Ocean Modelling* **2006,** *12*, 290-301.

[29] Al-Anezi, K.; Hilal, N. Scale formation in desalination plants: effect of carbon dioxide solubility. *Desalination* **2007,** *204,* 385-402

[30] Al-Anezi, K.; Somerfield, C.; Mee, D.; Hilal, N. K. Al-Anezi, C. Somerfield, D. Mee, N. Hilal, Parameters affecting the solubility of carbon dioxide in seawater at the conditions encountered in MSF desalination plants, Desalination **2008,** *222,* 548-571

[31] Rahbari-Sisakht, M.; Ismail, A. F.; Rana, D.; Matsuura, T.; Emadzadeh, D. Carbon dioxide stripping from water through porous polysulfone hollow fiber membrane contactor, Separation and Purification Technology **2013,** *108,* 119-123.

FIGURE CAPTIONS

Figure 1. (a) Schematic of Original E-CEM and (b) Schematic of Modified E-CEM.

Figure 2. (a) A pH profile comparison of seven polarity cycles measured for the modified E-CEM at 20 A (408 A/m^2 current density) as a function of time, 45 minute cycle, polarity A and (b) A pH profile comparison of seven polarity cycles measured for the modified E-CEM at 20 A (408 A/m^2 current density) as a function of time, 45 minute cycle, polarity B.

Figure 3. Average pH profiles for the original E-CEM as a function of time at 20 A (408 A/m^2 current density), polarity A (■) and polarity B (□) compared to the modified E-CEM at the same current density, polarity A (●) and polarity B (○).

Figure 4: Average electrical resistance profile comparison of seven polarity cycles measured for the modified E-CEM at 20 A (408 A/m^2 current density) as a function of time, 45 minute cycle, polarity A (●), 45 minute cycle, polarity B (○).

Figure 5: Electrochemical components that affect the overall conductivity of the module

Figure 6: Average electrical resistance profiles as a function of time measured for the original E-CEM and the modified E-CEM at 20 A (408 A/m^2 current density) and 45 minute cycles, modified E-CEM polarity A (●), polarity B (○), original E-CEM polarity A (■), polarity B (□).

Figure 7: A electrical resistance profile comparison of five polarity cycles measured for the original E-CEM at 20 A (408 A/m^2 current density) as a function of time, January 2011 [40 minute cycle, polarity A (□), polarity B (■)], April 2011 [45 minute cycle, polarity A (●), polarity B (○)], August 2011 [45 minute cycle, polarity A (▼), polarity B (▽)], January 2012 [45 minute cycle, polarity A (▲), polarity B (Δ)].

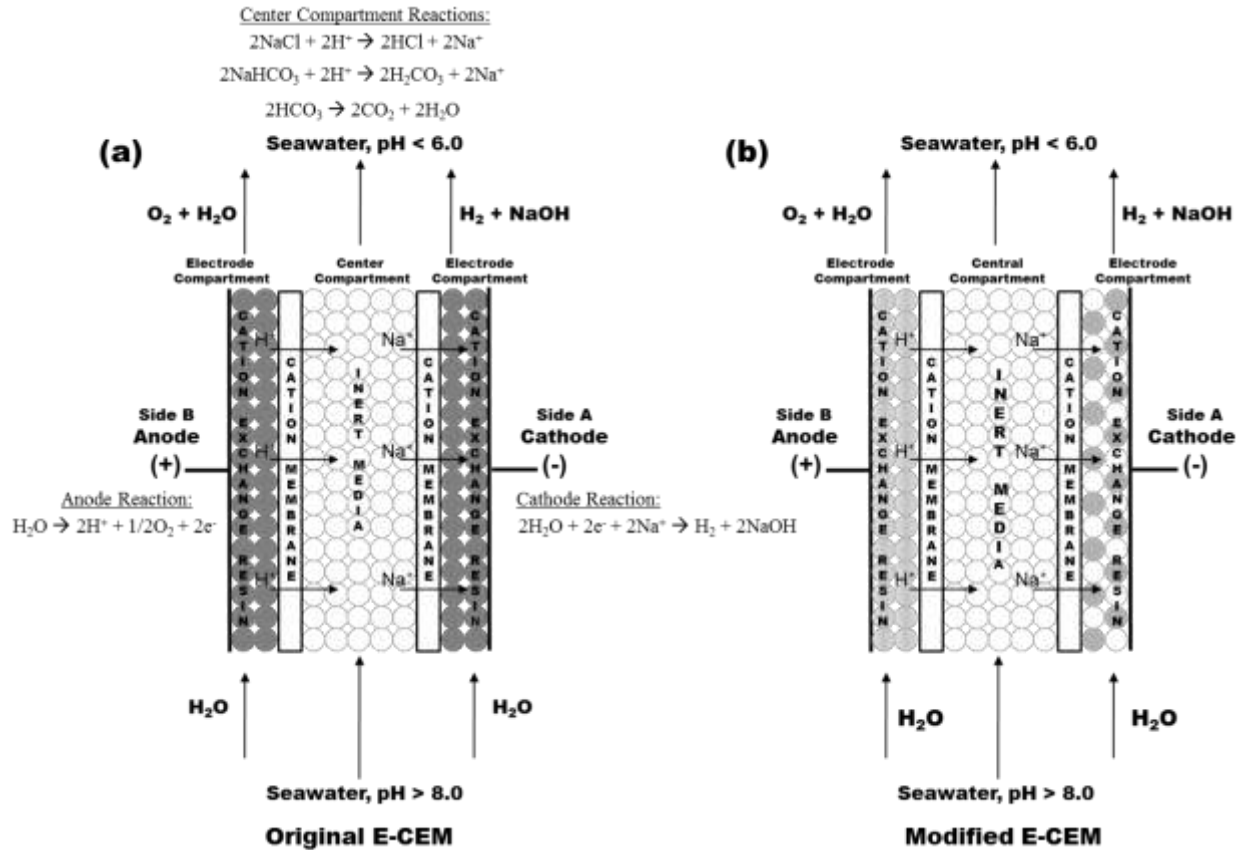**Figure 1.** (a) Schematic of Original E-CEM and (b) Schematic of Modified E-CEM.

Center Compartment Reactions:

$$2NaCl + 2H^+ \rightarrow 2HCl + 2Na^+$$

$$2NaHCO_3 + 2H^+ \rightarrow 2H_2CO_3 + 2Na^+$$

$$2HCO_3 \rightarrow 2CO_2 + 2H_2O$$

Anode Reaction:
$$H_2O \rightarrow 2H^+ + 1/2O_2 + 2e^-$$

Cathode Reaction:
$$2H_2O + 2e^- + 2Na^+ \rightarrow H_2 + 2NaOH$$

Figure 2. (a) A pH profile comparison of seven polarity cycles measured for the modified E-CEM at 20 A (408 A/m² current density) as a function of time, 45 minute cycle, polarity A and (b) A pH profile comparison of seven polarity cycles measured for the modified E-CEM at 20 A (408 A/m² current density) as a function of time, 45 minute cycle, polarity B.
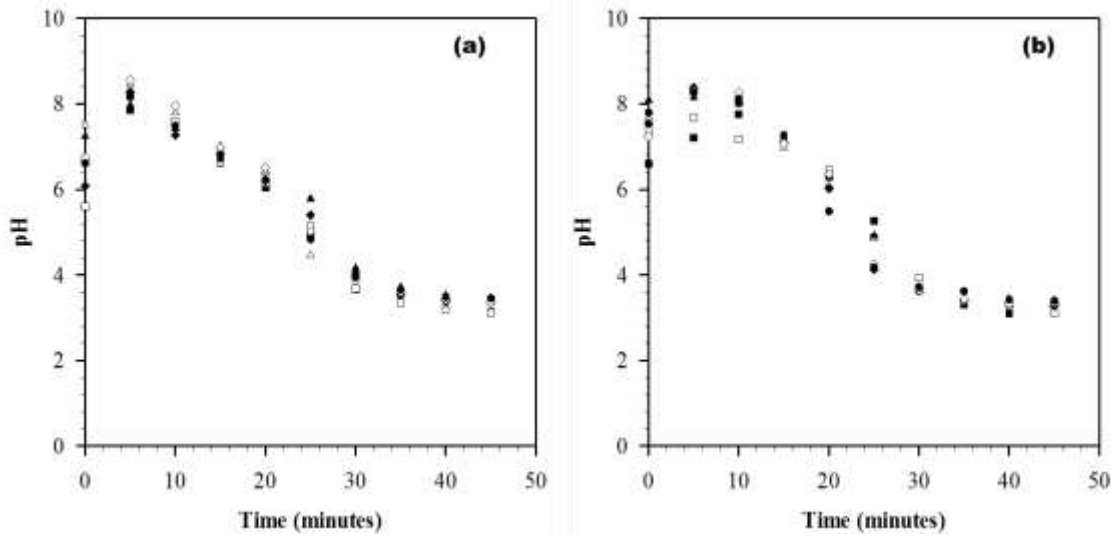
Figure 3. Average pH profiles for the original E-CEM as a function of time at 20 A (408 A/m^2 current density), polarity A (■) and polarity B (□) compared to the modified E-CEM at the same current density, polarity A (●) and polarity B (○).
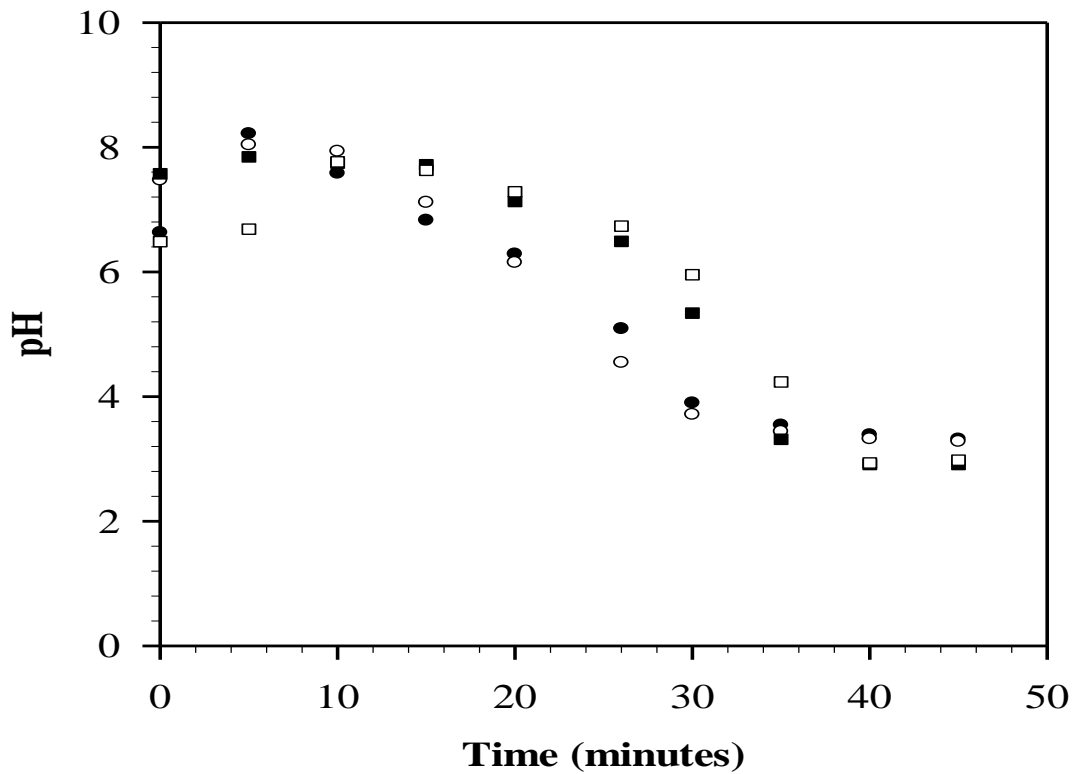
Figure 4: Average electrical resistance profile comparison of seven polarity cycles measured for the modified E-CEM at 20 A (408 A/m^2 current density) as a function of time, 45 minute cycle, polarity A (●), 45 minute cycle, polarity B (○).
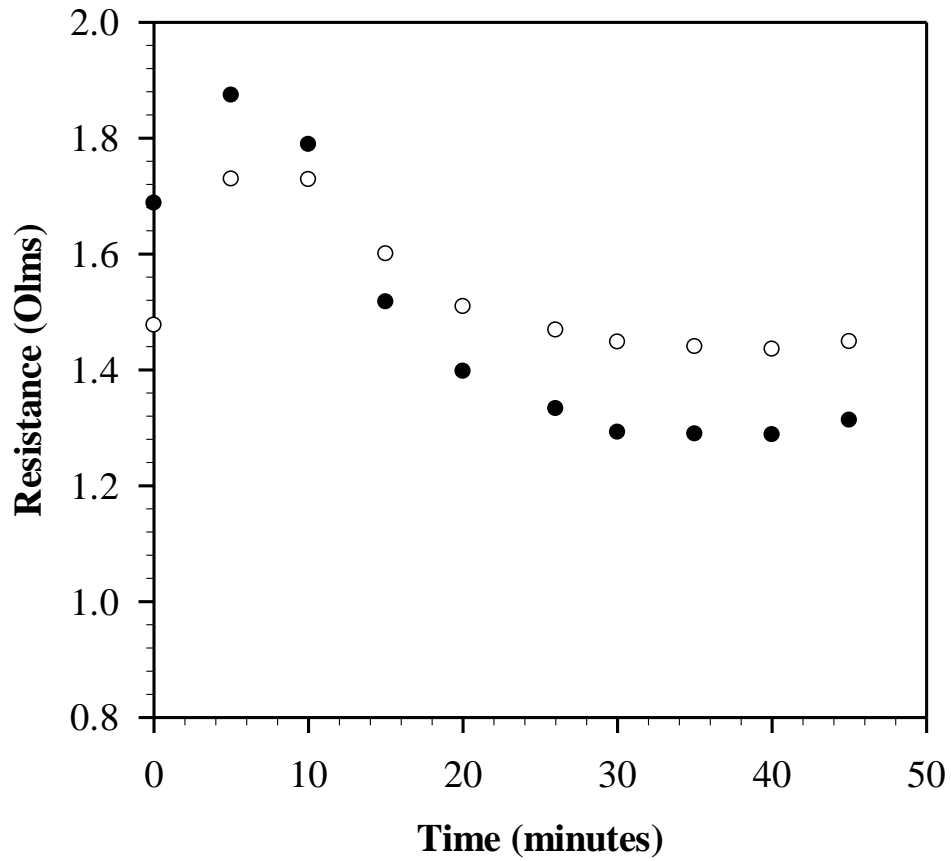

Figure 5: Electrochemical components that affect the overall conductivity of the module.
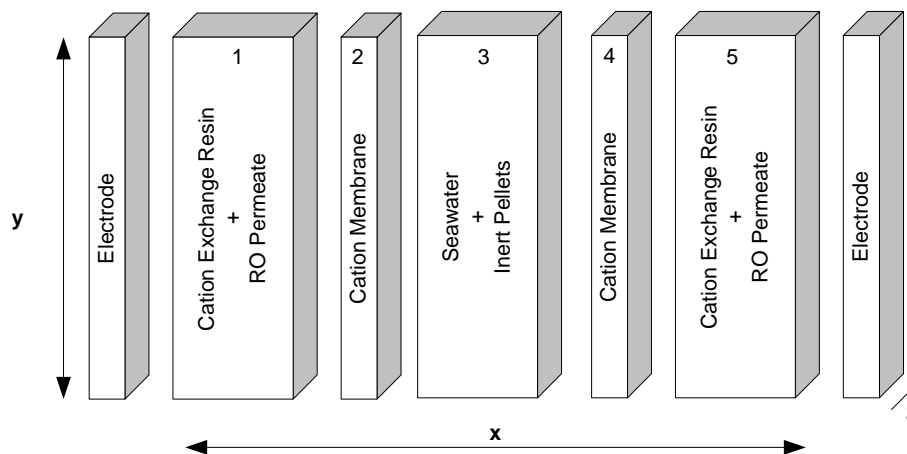
Figure 6: Average electrical resistance profiles as a function of time measured for the original E-CEM and the modified E-CEM at 20 A (408 A/m^2 current density) and 45 minute cycles, modified E-CEM polarity A (●), polarity B (○), original E-CEM polarity A (■), polarity B (□).
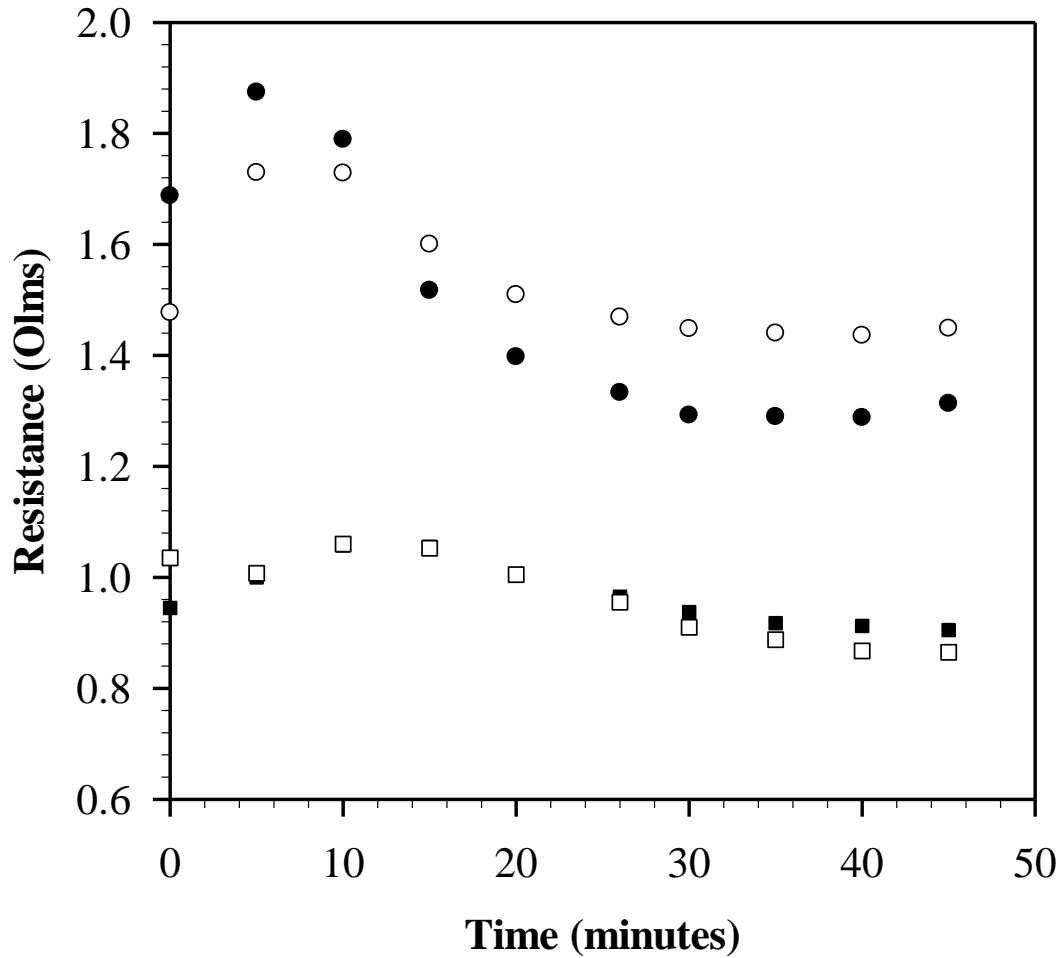
Figure 7: A electrical resistance profile comparison of five polarity cycles measured for the original E-CEM at 20 A (408 A/m² current density) as a function of time, January 2011 [40 minute cycle, polarity A (□), polarity B (■)], April 2011 [45 minute cycle, polarity A (●), polarity B (○)], August 2011 [45 minute cycle, polarity A (▼), polarity B (▽)], January 2012 [45 minute cycle, polarity A (▲), polarity B (△)].
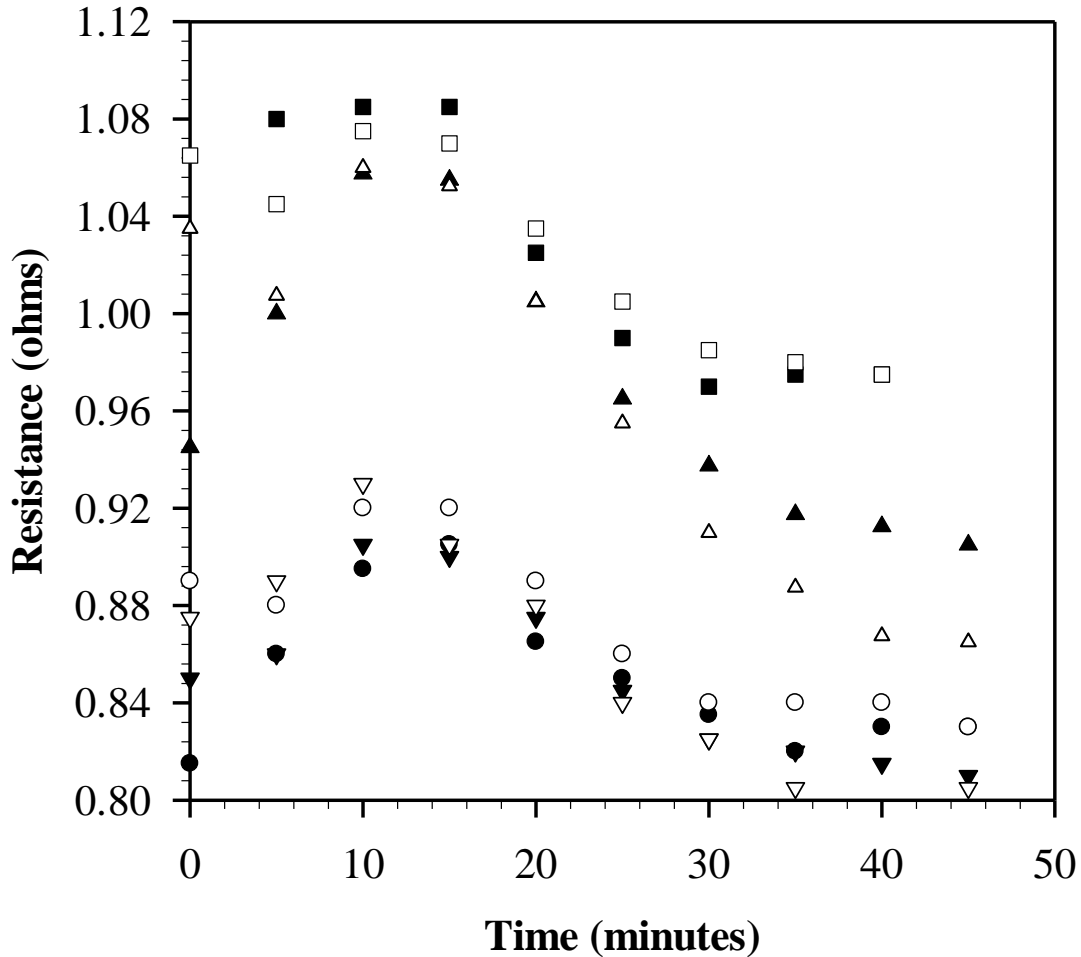
TABLE CAPTIONS

Table 1. The average measured values of effluent seawater pH, module current, voltage, and resistance as a function of time using the modified E-CEM during consecutive 45 minute polarity cycles at an applied module current of 20 A (408 A/m^2 current density).

Table 2. CO_2 Degassed Samples from Acidification of KW seawater.

Table 1. The average measured values of effluent seawater pH, module current, voltage, and resistance as a function of time using the modified E-CEM during consecutive 45 minute polarity cycles at an applied module current of 20 A (408 A/m^2 current density).

Time (minutes)	Amps	Volts	Resistance	pH	Conductivity	Polarity
0	18.2	30.5	1.69	6.63	0.0021	A
5	16.7	31.0	1.87	8.21	0.0019	A
10	17.4	31.0	1.80	7.58	0.0020	A
15	19.9	30.2	1.52	6.82	0.0024	A
20	20.0	27.9	1.40	6.29	0.0026	A
25	20.0	26.6	1.33	5.10	0.0027	A
30	20.0	25.8	1.30	3.90	0.0028	A
35	20.0	25.8	1.29	3.54	0.0028	A
40	20.0	25.8	1.29	3.40	0.0028	A
45	20.0	26.3	1.31	3.32	0.0028	A
0	20.0	29.5	1.48	7.47	0.0024	B
5	18.0	31.0	1.73	8.04	0.0021	B
10	18.0	31.0	1.73	7.93	0.0021	B
15	19.4	31.0	1.60	7.11	0.0023	B
20	20.0	30.2	1.51	6.15	0.0024	B
25	20.0	29.4	1.47	4.55	0.0025	B
30	20.0	29.0	1.48	3.77	0.0025	B
35	20.0	28.8	1.44	3.43	0.0025	B
40	20.0	28.7	1.43	3.32	0.0025	B
45	20.0	29.0	1.45	3.28	0.0025	B

Table 2. CO₂ Degassed Samples from Acidification of KW seawater.

Seawater Sample Date	Seawater (pH)	Vacuum Pump	Vacuum pressure inches Mercury	(%) Reduction of CO_2 by Coulometery	(%) CO_2 Gas by TCD (onsite)	(%) CO_2 in Gas by (Independent Evaluations)
January 2011	8.03	No vacuum	No pressure	0	-----	-----
	3.63	No vacuum	No pressure	48	-----	-----
April 2011	8.26	No vacuum	No pressure	0	-----	------
	3.82	Rotary Vain	30	92	-----	-----
January 2012	8.18	No vacuum	No pressure	0		
	3.67	diaphragm	29.1	63		
	3.46	diaphragm	29.1	66	63	
	3.44	diaphragm	29.1			65
	3.66	diaphragm	29.1			63
	3.81	Rotary vain	30.5	85		